REPORT DOCUMENTATION PAGE

Form Approved
OMB No. 0704-0188

1. REPORT DATE *(DD-MM-YYYY)*	**2. REPORT TYPE**	**3. DATES COVERED** *(From - To)*
07-06-2012	Conference Paper	

4. TITLE AND SUBTITLE

A comparison of the performance of 1st order and 2nd order turbulence models when solving the RANS equations in reproducing the liquid film length unsteady response to momentum flux ratio in Gas-Centered Swirl-Coaxial Injectors in Rocket Engine Applications

5a. CONTRACT NUMBER

5b. GRANT NUMBER

5c. PROGRAM ELEMENT NUMBER

6. AUTHOR(S)

L.A. Villasmil and A. Himansu

5d. PROJECT NUMBER

5f. WORK UNIT NUMBER
50260538

7. PERFORMING ORGANIZATION NAME(S) AND ADDRESS(ES)

Air Force Research Laboratory (AFMC)
AFRL/RQRC
10 E. Saturn Blvd.
Edwards AFB CA 93524-7401

8. PERFORMING ORGANIZATION REPORT NUMBER

9. SPONSORING / MONITORING AGENCY NAME(S) AND ADDRESS(ES)

Air Force Research Laboratory (AFMC)
AFRL/RQR
5 Pollux Drive
Edwards AFB CA 93524-7048

10. SPONSOR/MONITOR'S ACRONYM(S)

11. SPONSOR/MONITOR'S NUMBER(S)
AFRL-RZ-ED-TP-2012-156

12. DISTRIBUTION / AVAILABILITY STATEMENT

Distribution A: Approved for public release; distribution unlimited. PA# 12410.

13. SUPPLEMENTARY NOTES

ILASS Americas 2012, San Antonio, TX, 20-23 May 2012 and for publication in the ILASS Americas 2012 Conference Proceedings, December 2012.

14. ABSTRACT

In liquid rocket combustion devices, mixture formation is one of the most important processes because it determines combustion efficiency, stability, and heat transfer characteristics. The swirling gas and liquid flows in Gas-Centered Swirl-Coaxial Injectors (GCSC) injectors lead to high-quality atomization achieved but with some drawbacks of non-uniformity of flow intensity and mixture composition. We are currently performing numerical simulations in GCSC Injectors geometries that have exhibited some spray non-uniformities when tested at particular operating conditions. Based on validations of previous work in simulations of a round jet, we solve the unsteady RANS equations with the well-known VOF model for the handling of the liquid and gas phases while comparing the performance of two 1_{st} order turbulence models (k-ε and k-ω) and one 2_{nd} order turbulence model (RSM). The main objective is to evaluate their ability to reproduce the non-dimensional fuel (liquid) film length response to momentum flux ratio. Preliminary results indicate that the Reynolds Stress Model predictions are comparable to those obtained with the Standard k-ε model, nevertheless the former is capable of predicting some liquid-gas instabilities and shedding frequencies that the latter is not able to capture. When compared to the actual experiments, all turbulent models un-der-predict the liquid film length, but the performance of the Standard k-ω model is rather questionable.

15. SUBJECT TERMS

16. SECURITY CLASSIFICATION OF:			**17. LIMITATION OF ABSTRACT**	**18. NUMBER OF PAGES**	**19a. NAME OF RESPONSIBLE PERSON**
					Stephen A. Danczyk
a. REPORT	**b. ABSTRACT**	**c. THIS PAGE**			**19b. TELEPHONE NUMBER** *(include area code)*
Unclassified	**Unclassified**	**Unclassified**	SAR	14	N/A

A comparison of the performance of 1ST order and 2ND order turbulence models when solving the RANS equations in reproducing the liquid film length unsteady response to momentum flux ratio in Gas-Centered Swirl-Coaxial Injectors in Rocket Engine Applications.

L. A. Villasmil*
Department of Mechanical Engineering Technology
Rochester Institute of Technology
Rochester, NY 14623-5604 USA

A. Himansu
Air Force Research Laboratory
Aerophysics Branch
10 E. Saturn Blvd.
Edwards AFB, CA 93524 USA

Abstract

In liquid rocket combustion devices, mixture formation is one of the most important processes because it determines combustion efficiency, stability, and heat transfer characteristics. The swirling gas and liquid flows in Gas-Centered Swirl-Coaxial Injectors (GCSC) injectors lead to high-quality atomization achieved but with some drawbacks of non-uniformity of flow intensity and mixture composition. We are currently performing numerical simulations in GCSC Injectors geometries that have exhibited some spray non-uniformities when tested at particular operating conditions. Based on validations of previous work in simulations of a round jet, we solve the unsteady RANS equations with the well-known VOF model for the handling of the liquid and gas phases while comparing the performance of two 1st order turbulence models (k-ε and k-ω) and one 2nd order turbulence model (RSM). The main objective is to evaluate their ability to reproduce the non-dimensional fuel (liquid) film length response to momentum flux ratio. Preliminary results indicate that the Reynolds Stress Model predictions are comparable to those obtained with the Standard k-ε model, nevertheless the former is capable of predicting some liquid-gas instabilities and shedding frequencies that the latter is not able to capture. When compared to the actual experiments, all turbulent models under-predict the liquid film length, but the performance of the Standard k-ω model is rather questionable.

*Corresponding author: larry.villasmil@rit.edu

Introduction

Gas-Centered Swirl Coaxial (GCSC) injectors are of interest for rocket applications, especially in engines using liquid hydrocarbon fuels and oxidizer-rich preburning cycles. Previous studies on evaluating possible design criteria have found that ensuring good atomization performance while allowing some throttling of the engine requires keeping their operation above a certain gas-to-liquid momentum flux ratio. Nevertheless, uniformity, in space and time, of the resulting spray is also important for successful operation. Under certain conditions, GCSC injectors have been found to produce non-uniform sprays, particularly atomization departing from the centerline and also pulsing [1].

In recent years, the Air Force Research Laboratory has focused on fundamental studies of GCSC injectors that have found some evidence indicating that observed spray non-uniformities might be linked to the relationship between the liquid film and spray behavior [1]. In general, evaluating the performance of GCSC injectors through experimentation and testing is relatively time consuming and requires significant economic resources. Multiple geometry and flow rate combinations (momentum flux ratios) need to be reviewed and compared. Therefore, having the ability to predict injector performance using modeling and simulations can reduce the cost of rocket engine development [2]. In terms of injector design, such cost reduction can be significant if current or newly developed models are validated by replicating the GCSC injectors test data with some degree of accuracy, particularly, if the numerical models have a degree of generality.

To the best of our knowledge, the most recent attempt to fully model the behavior of gas-centered swirl coaxial fuel injectors is due to Trask et al. [3]. The authors implemented an Eulerian two-phase model to represent the liquid and gas interactions in the injector as well as the atomization processes occurring at the rough interface. They found that limiting turbulent mixing via the Schmidt number predictions could fairly replicate the experiments but concluded that the actual mechanism for limiting the mixing should be coming from the turbulence closures and not from the liquid flux closure. They used a modified form of the two equation k-ε model as the former and indicated that the stabilizing effect that swirl has on turbulence cannot be resolved through a linear eddy viscosity model, suggesting that more appropriate models, such as an algebraic or differential Reynolds Stress model could potentially yield similar results while using more typical values for the mass transfer constants.

Motivation – Round Jet Experiment Replication

As part of the investigation, we simulated a turbulent round jet chamber experiment [4] validating the referenced report findings regarding the performance of the k-ε model, see Figure 1. Nevertheless, we hypothesized that turbulence models predicting a lower spreading rate would perform better in replicating the Gas-Centered Swirl-Coaxial Injectors experiments. Therefore, we compared the predictions of several turbulence model combinations focusing on the spreading rate of the jet near the exit. The models that predict the lowest average spreading rate in the non-dimensional axial distance equivalent to the injector length are the k-ω and the Reynolds stress model (RSM), see Figure 2.

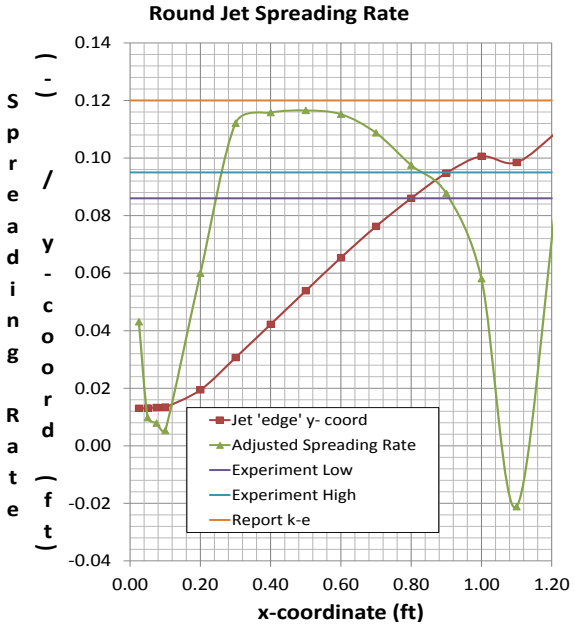

Figure 1. Round Jet Spreading Rate [4].

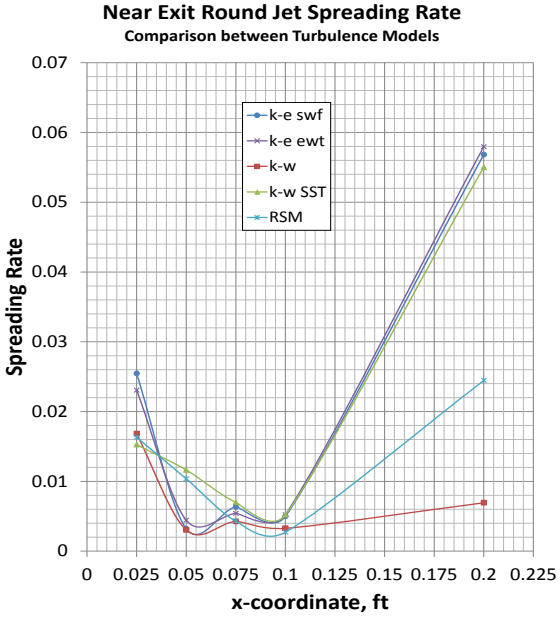

Figure 2. Near Exit Round Jet Spreading Rate.

Numerical Procedure

We are solving the unsteady RANS equations with the well-known Volume of Fluid (VOF) model for the handling of the liquid and gas phases while comparing the performance of two 1st order turbulence models (Standard k-ε and k-ω) and one 2nd order model (Reynolds Stress Model or RSM). For the near wall approach to turbulence, we are using the enhanced wall treatment (EWT) and the standard wall functions (SWF).

Geometry, Grid Detail, and Boundary Conditions.

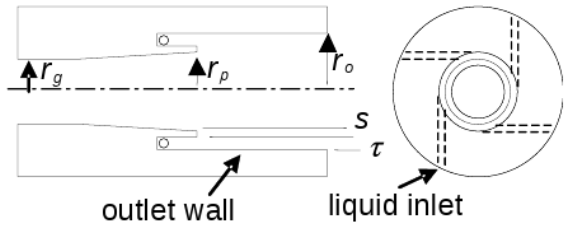

Name	r_o (mm)	τ (mm)	r_g (mm)	s (mm)
ONPNTN	9.525	1.651	6.350	1.524

Figure 3. Actual Injector Cup Geometry.

The ongoing numerical analysis has focused on the ONPNTN injector cup geometry depicted in Figure3. The modeling domain includes an enlarged inlet port and an extended exit 'chamber', Figure 4. The intent of adding an inlet port is to smooth out any perturbation associated with the mass flux boundary condition while any possible backflow from the liquid recirculation at the injector lip is not numerically limited. Similarly, the objective of extending the injector beyond the minimum geometry is to isolate the injector exit from the recirculation flow that normally occur in these round jet related applications (recirculation flow does not carry information on turbulent quantities) minimizing the 'numerical reflection' effect that occurs when prescribing the pressure at the outlet of the domain.

Regarding boundary conditions, all solid surfaces are defined as no-slip walls, the 'water' is injected into the liquid port by prescribing the liquid velocity profile at the inlet including the swirl velocity when applicable, the 'gas' enters the domain by prescribing the mass flux profile (the product of the density and the axial velocity) and turbulent quantities at the gas post, and the static pressure at the outlet.

Discretization Scheme and Solver Algorithm

To define the discretization scheme to be used, we performed multiple tests (starting with a simple case of an inkjet printer nozzle [5]) to evaluate the stability of the droplets and liquid interface during unsteady simulations and found that the second order "Quick" scheme works best, particularly when combined with the "Geo-Reconstruct" scheme for the Volume of Fluid (VOF) interface tracking. Other discretization schemes, particularly the first order type are extremely dissipative and smear considerably the interface.

In terms of the solver algorithms, using the "Geo-Reconstruct" scheme for the VOF requires the use of the explicit solver to advance the solution in time. The drawback of using the explicit solver is that such approach required much smaller time steps to guarantee that a converged and stable solution is obtained during each fractional time step (Global Courant number criteria [5]). In theory, this limitation can be overcome by using the implicit approach which is more stable and allows flexibility in terms of the time step size. Nevertheless, during the liquid-gas interface stability evaluations mentioned above we found that this approach also exhibits smearing of the interface due to artificial numerical dissipation as the flow time progresses in addition to being more computationally expensive (when compared to the explicit solver with equal time steps for a specific test case). Therefore, ongoing simulations are being performed with the explicit approach and fractional step temporal discretization with non-iterative time advancement acknowledging that given the high velocities of the gas phase coupled with the fine grid resolution required, the criteria for stability demands a time step size in the order of 10^{-7} s.

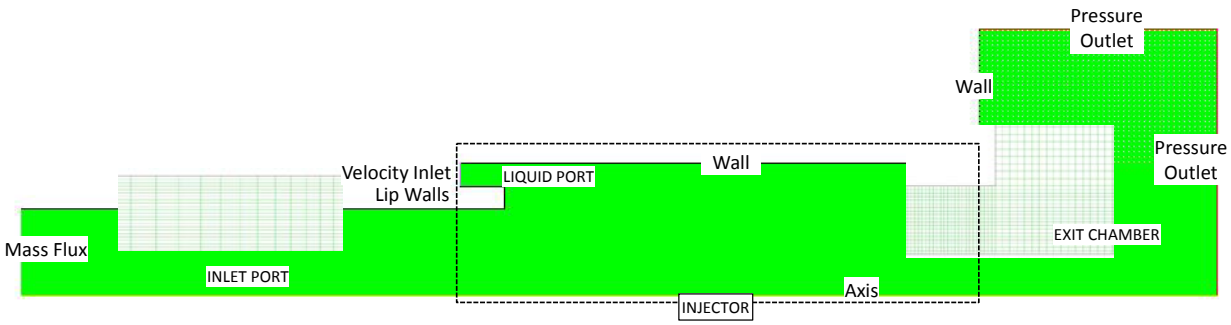

Figure 4. ONPNTN Injector Geometry with Extended Inlet/Outlet Domains (grid enlargements shown)

Grid Validation - Grid Convergence Analysis

To estimate an appropriate mesh size for all simulations, a grid independence study following the work of Roache [6] was done for a nitrogen mass flow rate of 0.0567 kg/s at operating conditions (no liquid injection). In this particular case rather than paying attention to the values themselves, we focused on how they changed as the mesh was refined particularly in the spreading zone of the jet near the wall of the injector. Figure 5 presents the mesh progression use for the simulations. Simulations performed with the standard k-ε model were performed in predominantly uniform grids as depicted in Figure 5a. Simulations performed with the k-ω and RSM models were performed in a mixed mesh with local refinement along the injector cup (liquid port and injector lip), Figure 5b.

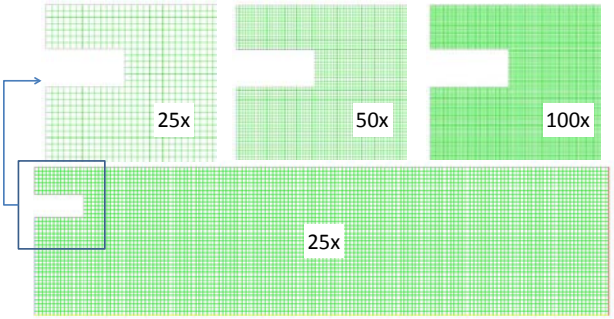

Figure 5a. Uniform Mesh Progression

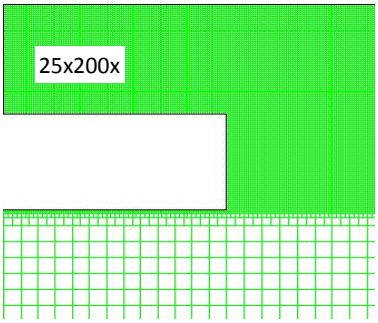

Figure 5b. Mixed Meshing - Localized Refinement

Figure 5.
Mesh Progression (2D), 25x~250 μm; 200x ~ 30 μm

Figure 6a and 6b show the axial and radial velocity profiles predicted for the gas leaving the injector with the standard k-ε model. The criteria established by Roache [6] to evaluate methodically the grid resolution is the use of the Grid Convergence Index or GCI. Based on the axial velocity, the grid size '50x' is already satisfactory as the GCI is only 1.4%. On the other hand, the resolution of the radial velocity requires a finer grid, the grid size '100x' was selected as further refinement to '200x' results in a GCI of 1.2%. In terms of turbulent kinetic energy and dissipation, Figures 6c and 6d, the GCI is 0.27% and 0.60% respectively.

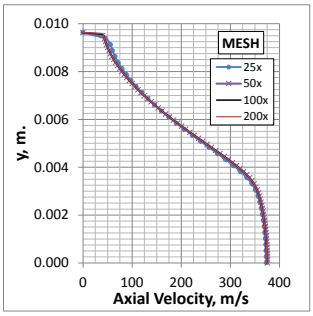

Figure 6a.

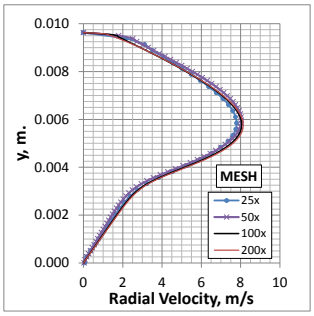

Figure 6b

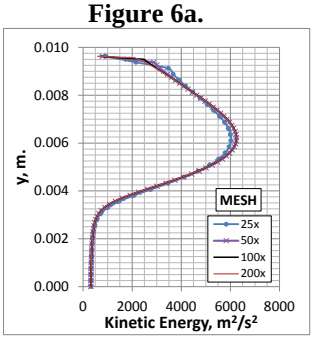

Figure 6c

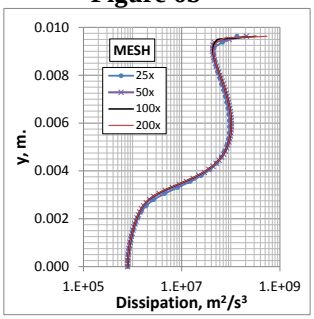

Figure 6d

Figure 6. Grid Independent Analysis for the Standard k-ε turbulence model case.

A similar analysis was conducted to establish the base meshing for the cases to be run with the Standard k-ω and RSM models. Figure 7a and 7b show the axial and radial velocity profiles predicted for the gas within the injector (roughly in the middle section) and the standard k-ω model. The grid size '50x' is again already satisfactory as the GCI is only 0.86%. On the other hand, the GCI for the radial velocity is 14%, a rather large value, requiring further refining with the grid size '100x' deemed acceptable as the projected GCI for going to the '200x' size is 2.75%. In terms of turbulent kinetic energy and specific dissipation, Figures 7c and 7d, the GCI was already 2.7% and 1.8% respectively. For the actual mesh used for the simulations, '25x200x', the GCI ranges from 0.46% to 3.39%. Comparable results were obtained for the solutions with the RSM model.

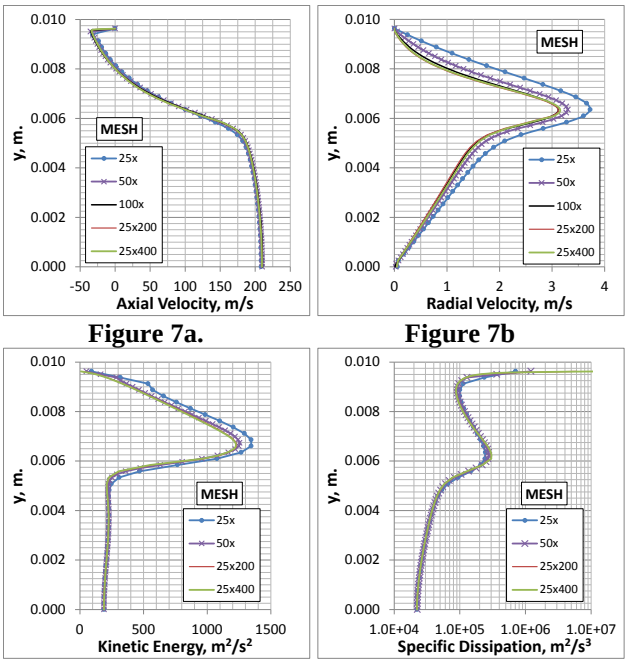

Figure 7a. **Figure 7b**

Figure 7c **Figure 7d**

Figure 7. Grid Independent Analysis for the Standard k-ω turbulence model case.

Preliminary Results

Volume of Fluid Contour Plots

Figures 8, 9 and 10 which appear at the end of this paper present the liquid volume fraction predictions for each turbulence model combination, no swirl and swirl. To the naked eye, it is clear that the Standard k-ω model is the one that promotes larger turbulent mixing as there is no significant liquid film length. Similarly, all predictions indicate that the addition of swirl appears to stabilize the liquid-gas interface extending the liquid film length with the exception of the Standard k-ω model. The most relevant aspect is the fact that the predictions with the Standard k-ε turbulence model appear to have a better definition of the liquid-gas interface than any other of the two models. Nevertheless, this fact is most likely related to the discretization scheme than the turbulence model itself. In Figure 11 (found after the text of the paper), we compare the solutions obtained with Standard k-ε turbulence model with those obtained with exactly the same modeling and discretization approach except for the advancement of the VOF tracking interface. The liquid film length and interface definition is comparable in all time frames presented with the exception that all ligaments and droplets are dissipated when the Geo-reconstruct discretization scheme is not used.

Non-Dimensional Liquid Film Length.

Based on the water VOF contours predicted by each turbulence model combination, we estimated the non-dimensional film length by averaging the film length of random time frames per each simulation. Table 1 presents a good estimate of the non-dimensional film length ratio calculated as outlined in Lightfoot [7] including the standard deviation.

Overall the predictions are well short of the values observed in the experiments, see Figure 12. Regarding the effect of the turbulence model on the predictions of the film length, the RSM model and the Standard k-ε appears to be in agreement. Both indicate that the addition of swirl increases the film length. On the other hand, the predictions of the Standard k-ω model are completely opposite indicating that the effect of the swirl is to reduce significantly the film length.

MODEL	L/τ (σ)
k-ε, no swirl	0.67 (0.37)
k-ε, swirl (Geo-reconstruct)	3.50 (0.57)
k-ε, swirl (Second Order Upwind)	4.21 (0.48)
k-ω, no swirl	1.12 (0.83)
k-ω, swirl	0.60 (0.74)
RSM, no swirl	1.36 (0.83)
RSM, swirl	3.14 (1.27)

Table 1. Non-dimensional predicted liquid film length

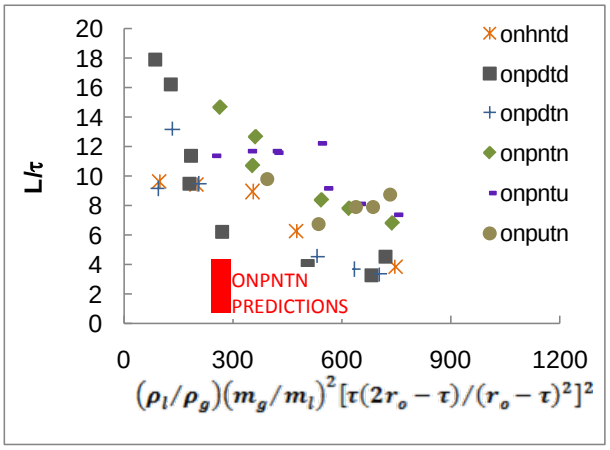

Figure 12. Non-dimensional film length vs. MFR [7]

Unsteadiness Analysis

Injector Exit Instantaneous mass flow rate predictions

The reasoning behind analyzing and comparing the mass flow predictions among turbulence models is that the magnitude of such flow rate is directly correlated with the amount of liquid that instantaneously crosses the exit plane of the injector. Due to the fact that the liquid is roughly 1000 times more dense, any small/large ligament or droplet will generate a 'spike' in the mass flow rate signal that is essentially liquid. Upon observation of the unsteadiness predicted for the behavior of the liquid-gas interface in preliminary runs, it is more certain that the magnitude of such spikes is correlated with the size of the ligaments predicted to

shed from the liquid-gas interface. One of the significant aspects observed in the experiments [7] regarding the behavior of the interface is the presence of low frequency pulsations. Such pulsations would significantly affect the performance of the injector in the actual application; hence the importance of exploring the ability of the numerical modeling in predicting such unsteadiness.

Figure 13 presents the comparison among predictions for the swirl versus no swirl case for the Standard k-ε turbulence model with the EWT approach as near wall treatment. There is no significant difference in the signals. Both present the highly intermittent nature of the liquid droplets or ligaments leaving the injector.

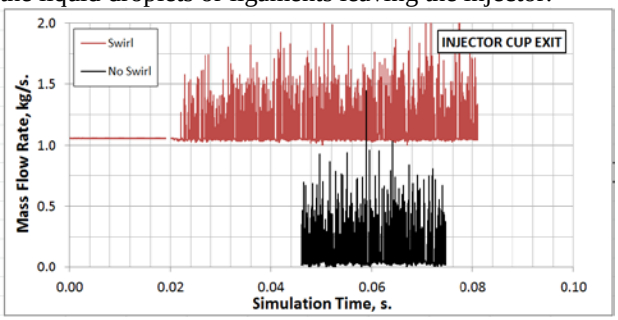

Figure 13. Injector Exit Instantaneous mass flow rate predictions, Standard k-ε with ewt turbulence model. mg = 0.0567 kg/s, ml=0.0327 kg/s, Vs ~3.9 m/s; Po ~ 104 kPa. (MFR ~ 280)

Figure 14 presents the predictions for the swirl case when comparing discretization methods for tracking the interface, Geo-reconstruct versus Second Order Upwind (SOU) schemes, using the Standard k-ε/EWT turbulence model combination. The 'SOU' simulation started as a 'Geo' simulation but was switched to the 'SOU' at a flow simulation time of 0.023 s. It is clear that the most relevant aspect is the 'damping' effect of the 'Quick' scheme in the amount of mass flow rate 'spikes' and their magnitude in the time sequence.

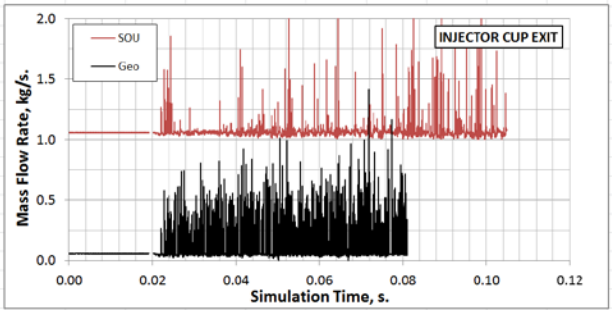

Figure 14. Injector Exit Instantaneous mass flow rate predictions, Standard k-ε with ewt turbulence model. Geo reconstruct versus Second Order Upwind discretization approach for the VOF. mg = 0.0567 kg/s, ml=0.0327 kg/s, Vs ~ 3.9 m/s; Po ~ 104 kPa. (MFR ~ 280)

To scrutinize further the Injector Exit Instantaneous mass flow rate predictions we performed a Fast Fourier Transform (FFT) on both signals. Figure 15 presents both frequency spectrums. As expected, the 'Geo' predictions create a richer spectrum in terms of amplitudes particularly on the higher frequency end. Nevertheless, neither signal shows a significant 'resonant' or 'peak' value that could point to a predominant unsteady phenomenon indicative of liquid-interface shedding. Given the sampling size and the time step of the calculations, 10^{-7} s, the frequency bins are 19.07 Hz.

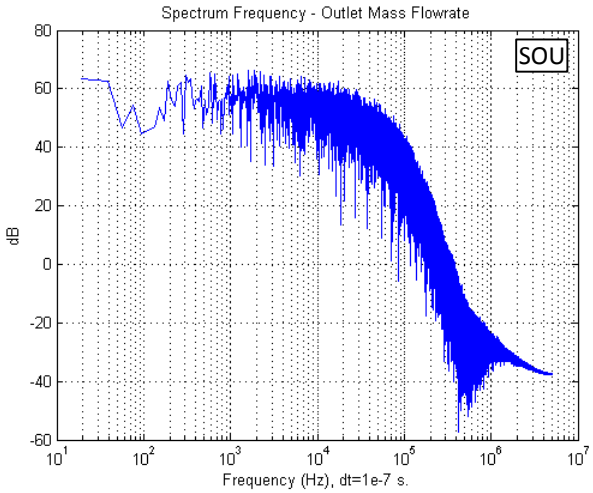

Figure 15a. Frequency spectrum diagram, VOF 'SOU' discretization.

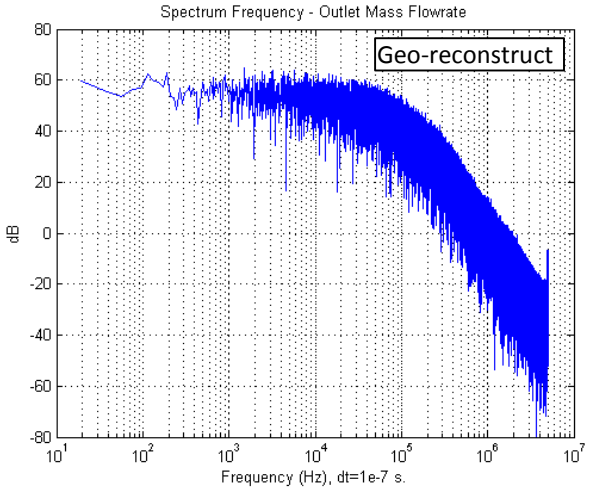

Figure 15b. Frequency spectrum diagram, VOF 'Geo-Reconstruct' discretization.

Figure 15. Comparing frequency spectrum diagrams of the Injector Exit Instantaneous mass flow rate predictions as signal for the swirl case, Standard k-ε with ewt turbulence model.

Figure 16 presents the predictions using the Standard k-ω turbulence model for both swirl and no swirl cases. At the beginning of both simulations the VOF discretization method is set to the 'Geo-reconstruct' scheme. The rest of variables are solved with the 'Quick' scheme. In both cases, swirl and no swirl, the VOF discretization scheme was switched to the 'Quick' quick at flow simulation times 0.014 s. and 0.017 s. respectively (while the liquid traveling interface has not left the injector liquid port yet). Both signals are relatively similar as they also show the 'damping' effect of the 'Quick' scheme in the amount and magnitude of the mass flow rate 'spikes' in the time sequence.

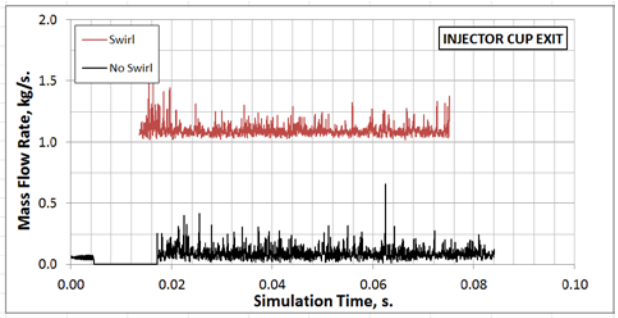

Figure 16. Injector Exit Instantaneous mass flow rate predictions, Standard k-ω turbulence model.
mg = 0.0567 kg/s, ml=0.0327 kg/s, Vs ~ 3.9 m/s;
Po ~ 104 kPa. (MFR ~ 260-270)

Similarly, to scrutinize further the Injector Exit Instantaneous mass flow rate predictions we performed a FFT on both signals, swirl and no swirl. Figure 17 presents both frequency spectrums. As expected, both predictions create a similar spectrum frequency distribution particularly on the higher frequency end. Nevertheless, in contrast to the Standard K-ε turbulence model predictions, the Standard K-ω model predictions create signals that show a significant 'resonant' or 'peak' value probably pointing to an unsteady phenomenon indicative of liquid-interface shedding. In the case of the no swirl, the signal presents two 'resonant' frequencies; one high value of approximately 2400 Hz and a medium value of 170 Hz. In the swirl case, the high value of 2400 is still present but the 170 Hz is 'damped' out. Like in the previous spectrum frequency analysis, the frequency bins are 19.07 Hz.

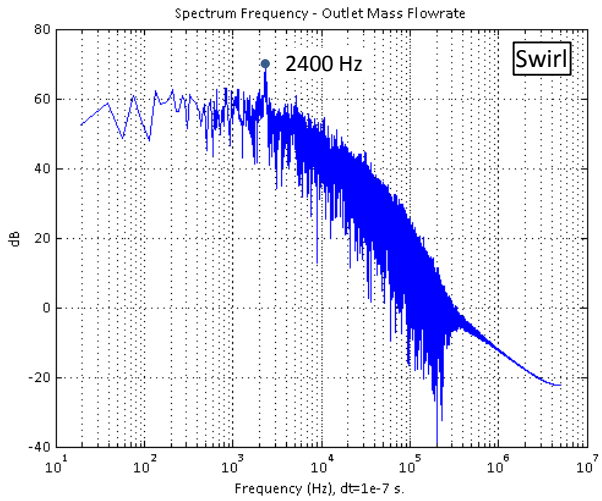

Figure 17a. Frequency spectrum diagram, Swirl Case.

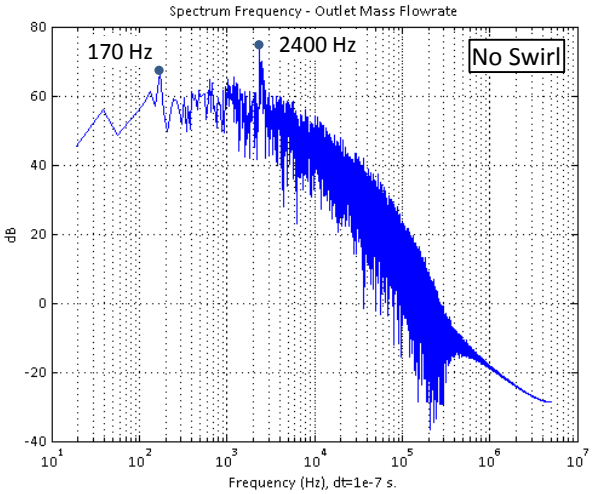

Figure 17b. Frequency spectrum diagram, No Swirl Case.

Figure 17. Spectrum frequency of the Injector Exit Instantaneous mass flow rate predictions.
Standard k-ω turbulence model

Figure 18 presents the predictions using the RSM model with the SWF functions for near wall treatment for both swirl and no swirl cases. At the beginning of both simulations the VOF discretization method is set to the 'Geo-reconstruct' scheme. The rest of variables are solved with the 'Quick' scheme. Like previous cases, the VOF discretization scheme was switched to the 'Quick' scheme soon after the simulations started, at a flow simulation time of 0.018 s. for the no swirl case and 0.011 s. for the swirl case (again while the liquid traveling interface has not left the injector liquid port). Both signals are relatively similar but in the swirl case the 'dampening' effect is accentuated. Although the time sequence is much shorter, it is clear that in the overlapping range the amount and magnitude of the

mass flow rate ‘spikes’ is significantly lower than the no swirl case.

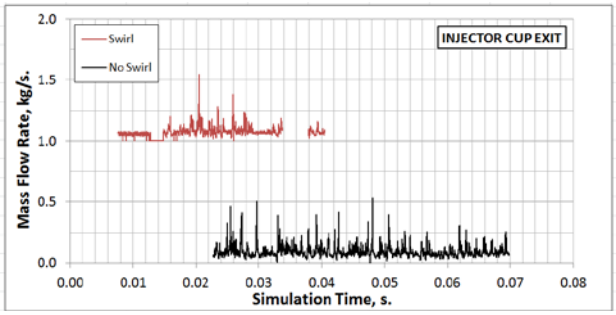

Figure 18. Injector Exit Instantaneous mass flow rate predictions, RSM/SWF turbulence model.
mg = 0.0567 kg/s, ml=0.0327 kg/s, Vs ~ 3.9 m/s;
Po ~ 104 kPa. (MFR ~ 270)

As we have done with previous mass flow rate signals, we performed a FFT on both signals, swirl and no swirl. Figure 19 presents both frequency spectrums. As expected, the no-swirl predictions indicate a richer spectrum in terms of amplitudes particularly on the higher frequency end. In contrast to the Standard K-ω turbulence model predictions, the RSM/SWF predictions only show significant ‘resonant’ or ‘peak’ values in the no swirl case at 340 Hz and 800 Hz. In the swirl case these values are ‘damped’ out, indeed there is no predominant frequency. Given the shorter time sequence, the sample size for the same time step size of 10^{-7} s. limited the frequency bins to 38.15 Hz. for the no swirl case and 79.30 Hz for the swirl case.

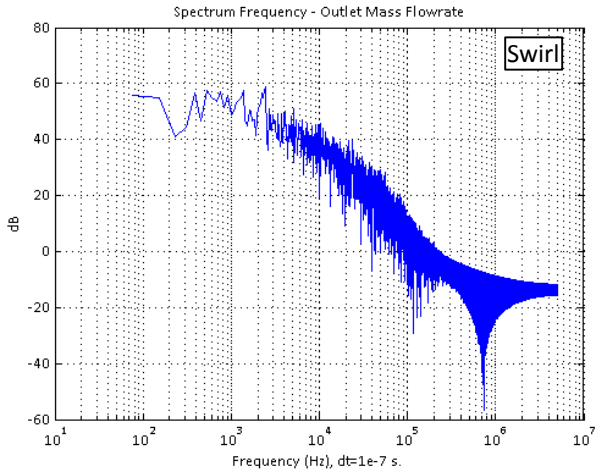

Figure 19a. Frequency spectrum diagram, Swirl Case.

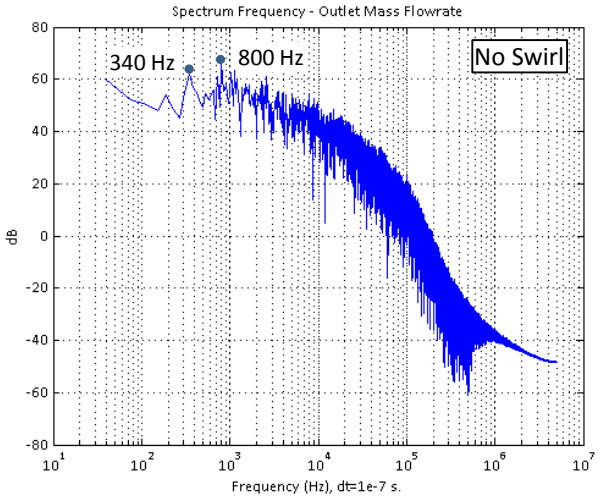

Figure 19b. Frequency spectrum diagram, No swirl case.

Figure 19. Spectrum frequency of the Injector Exit Instantaneous mass flow rate predictions.
RSM turbulence model with SWF.

Near Injector Lip VOF liquid fraction transient analysis

An alternative to analyze the mass flow rate fluctuations at the injector exit would be evaluating how the models predict the unsteadiness of the liquid film by ‘observing’ the liquid-gas interface behavior looking for intermittency and shedding. Given the small time step of the simulations, it would be extremely challenging to directly observe water VOF contour plots frame by frame (even as an animation). We decided to monitor the instantaneous liquid fraction in multiple locations within the domain with the hope that sudden changes in its value would be indicative of capturing oscillations and shedding of such interface.

Figure 20 compares the predicted water VOF near the injector lip that separates the liquid and gas ports, see insert on the Figure for the specific location, in the case of the Standard k-ω turbulence model for both cases swirl and no swirl. There are four clear ‘spikes’, values above 0.5 and/or near 1.0, for the no swirl case in the time sequence while there is only one single value above 0.5 in the swirl case. What is clearly significant is that the liquid VOF ‘spikes’ are clearly distinctive from the rest of the signal in the no swirl case with the first three separated by approximately the same time interval, 0.024-0.026 s., pointing to a possible shedding frequency predicted in the range of 38-42 Hz. The liquid VOF low predicted values for the swirl case, although with significantly more non-zero values along the time line than the no swirl case, do not indicate that the liquid-gas interface dips into the injector lip.

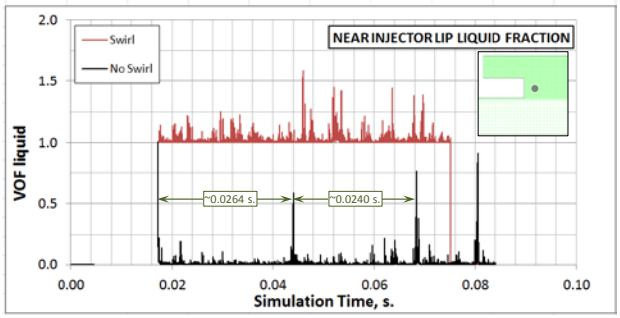

Figure 20. Near Injector Lip liquid VOF predictions, Standard k-ω turbulence model.
mg = 0.0567 kg/s, ml=0.0327 kg/s, Vs ~ 3.9 m/s;
Po ~ 104 kPa. (MFR ~ 260-270)

Similarly, Figure 21 compares the predicted water VOF near the injector lip for the RSM/SWF turbulence model combination for both cases swirl and no swirl. There are multiples 'spikes', values above 0.5 and/or near 1.0, for the no swirl case in the time sequence while there is literally none in the swirl case. These predictions are really in contrast to the Standard k-ω turbulence model predictions. The RSM/SWF model combination predicts that the addition of swirl would entirely suppress the presence of liquid near the injector lip. The presence of multiple 'spikes' in the no swirl case requires an analysis via FFT.

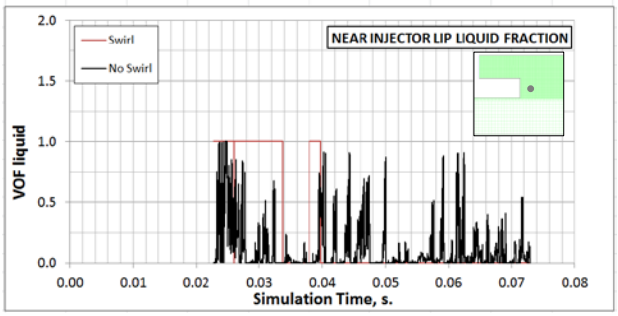

Figure 21. Injector Exit Instantaneous mass flow rate predictions, RSM/SWF turbulence model.
mg = 0.0567 kg/s, ml=0.0327 kg/s, Vs ~ 3.9 m/s;
Po ~ 104 kPa. (MFR ~ 270)

Figure 22 presents the frequency spectrum for a filtered near lip water VOF signal (only values above 0.5 were considered in the analysis). There are three clear dominant frequencies, 76 Hz., 340 Hz. and 880 Hz. The analysis is significant because it might be an indication of the liquid-gas interface 'dipping' into the injector lip at a frequency of 76 Hz. pointing to liquid shedding at this frequency value. The higher frequencies of 340 Hz. and 880 Hz. could be simply harmonics of the lower dominant frequency.

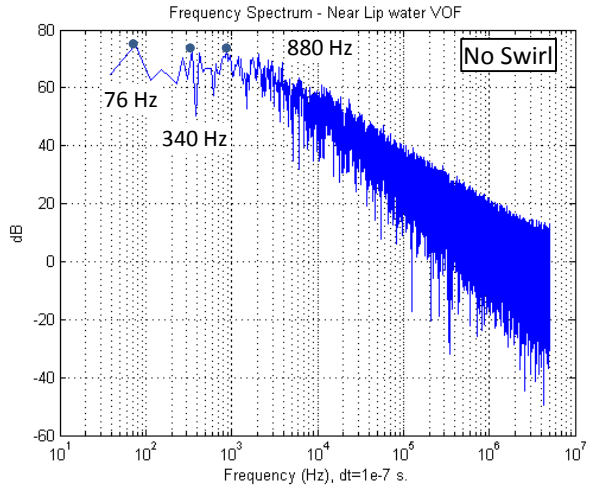

Figure 22. Near Lip water VOF Frequency Spectrum, RSM/SWF model predictions, no swirl case.

Discussion

When compared to the experiments, all predictions result in shorter film lengths. Nevertheless, the present analysis indicates that the Standard k-ω turbulence model clearly over-predicts the turbulent mixing at the liquid-gas interface. And either the Standard k-ε model or the RSM model perform better.

In terms on liquid film length intermittency and liquid-gas interface stability, The RSM model appears to be more consistent in predicting liquid shedding near the injector lip as the two methods employed to quantify such effect coincide in the estimated frequencies (340Hz and ~ 800Hz). All models predict that the effect of swirl is to 'damp out' liquid instability although the Standard k-ε predictions fail to indicate a predominant shedding frequency (based only on the analysis of the instantaneous mass flow rate at the exit).

The minimum predicted shedding frequency of 76 Hz is still relatively high when compared with observed frequencies of the order of 20 Hz. Nevertheless, we should point out that the simulations have not run long enough to be able to capture such low frequency values. Multiple tests have confirmed the stability criteria requiring a time step in the order of 10^{-7} s for the operating conditions of the injector.

One particular aspect we should mention is the effect of the discretization schemes. While using the 'Geo-reconstruct' scheme preserves better the liquid-gas interface, the added stability (in terms of computing stability) of the Second Order Upwind might be beneficial in exploring further the capabilities of the Reynolds Stress model in replicating the experiments.

In the next phase of this investigation, we will explore further the capabilities of the RSM model in replicating the experiments as the overall results indicate than it might be better suited to the problem at hand that the Standard k-ε. The Standard k-ω model appears not

be up to par with the much simpler and robust Standard k-ε.

Acknowledgement

This work has greatly benefited from the insights provided by Dr. Stephen A. Danczyk and Dr. Malissa D.A. Lightfoot, both of the Air Force Research Lab at Edwards AFB. Their expert knowledge of the physics of liquid atomization in gas-centered swirl co-axial injectors has influenced this paper. The first author acknowledges the financial support of this work by the Air Force Research Lab (USAF/ERC Incorporated) under Contract Number FA9300-06-C-0023.

References

1. Lightfoot M.D.A., Schumaker S.A., Danczyk S.A. *Atomization Uniformity in Gas-Centered Swirl-Coaxial Injectors*, DTIC ONLINE, 2010, accessed 2012 May 09, <http://www.dtic.mil/dtic/>.
2. Lightfoot M.D.A., Danczyk S.A. and Talley D.G. "Atomization Performance Predictions of Gas-Centered Swirl-Coaxial Injectors", DTIC ONLINE, 2007, accessed 2012 May 09, <http://www.dtic.mil/dtic/>..
3. Trask N., Perot J.B., Schmidt D.P., Meyer T., Lightfoot M.D.A. and Danczyk S.A. *Modeling of the Internal Two-Phase Flow in a Gas-Centered Swirl Coaxial Fuel Injector*. 48th AIAA Aerospace Sciences Meeting, 2010.
4. Bardina J.E., Huang P.G., Coakley T.J., "Turbulence Modeling Validation, Testing, and Development", April 1997, NASA Technical Memorandum 110446.
5. ANSYS FLUENT 12.0 Theory and User's Guide. April 2009.
6. Roache P.J. *Verification and Validation in Computational Science and Engineering*. Hermosa Publishers: Albuquerque, NM, 1998 (Chapter 5).
7. Lightfoot M.D.A., Danczyk S.A. and Talley D.G. "Scaling of Gas-Centered Swirl-Coaxial Injectors", DTIC ONLINE, 2008, accessed 2012 May 09, <http://www.dtic.mil/dtic/>..

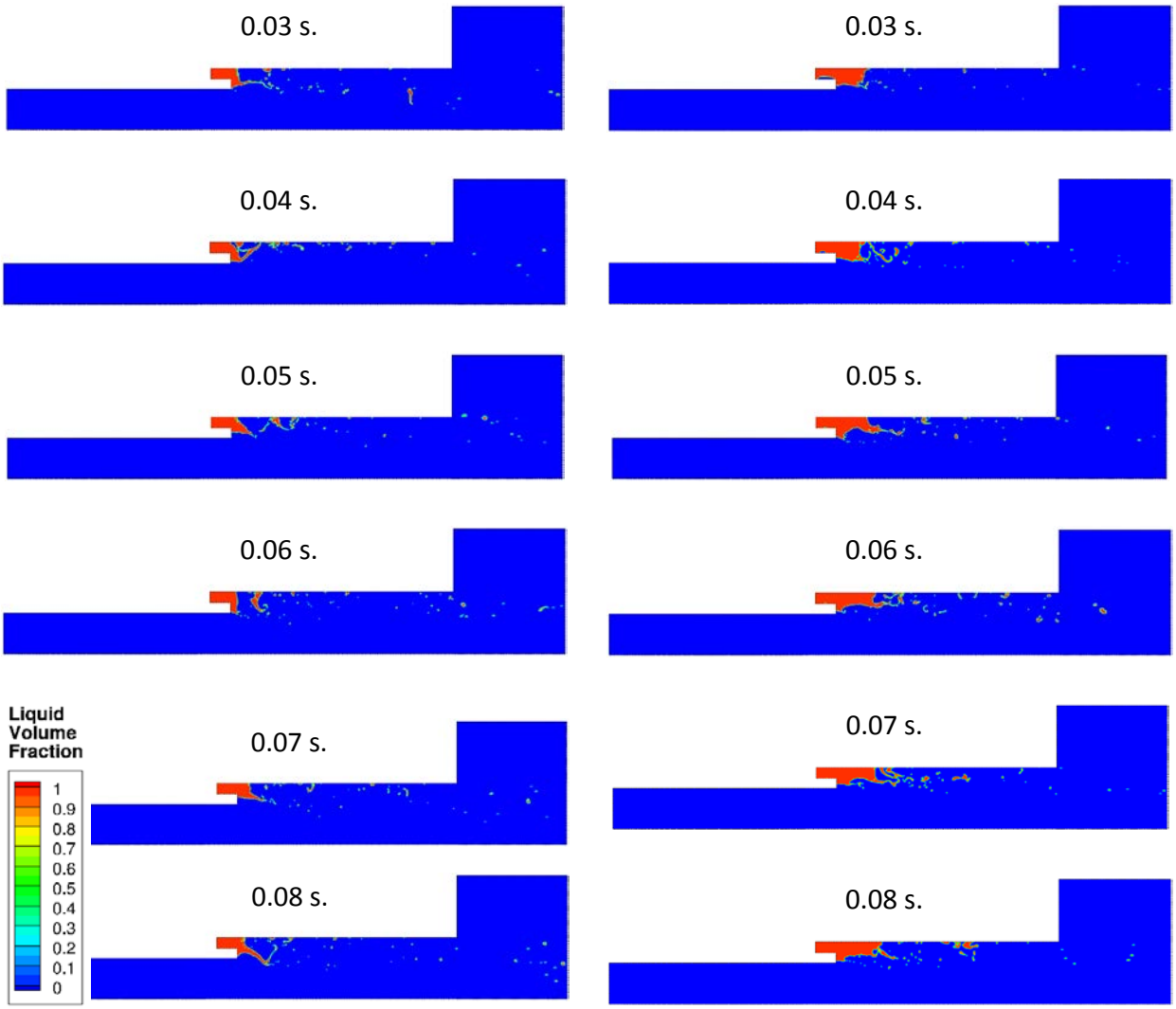

Figure 8. Contours of Liquid Volume Fraction. K-epsilon Turbulence Model.
No Swirl versus Swirl, mg = 0.0567 kg/s, ml=0.0327 kg/s, Vs ~ 3.9 m/s., Po ~ 104 kPa (MFR ~ 270)

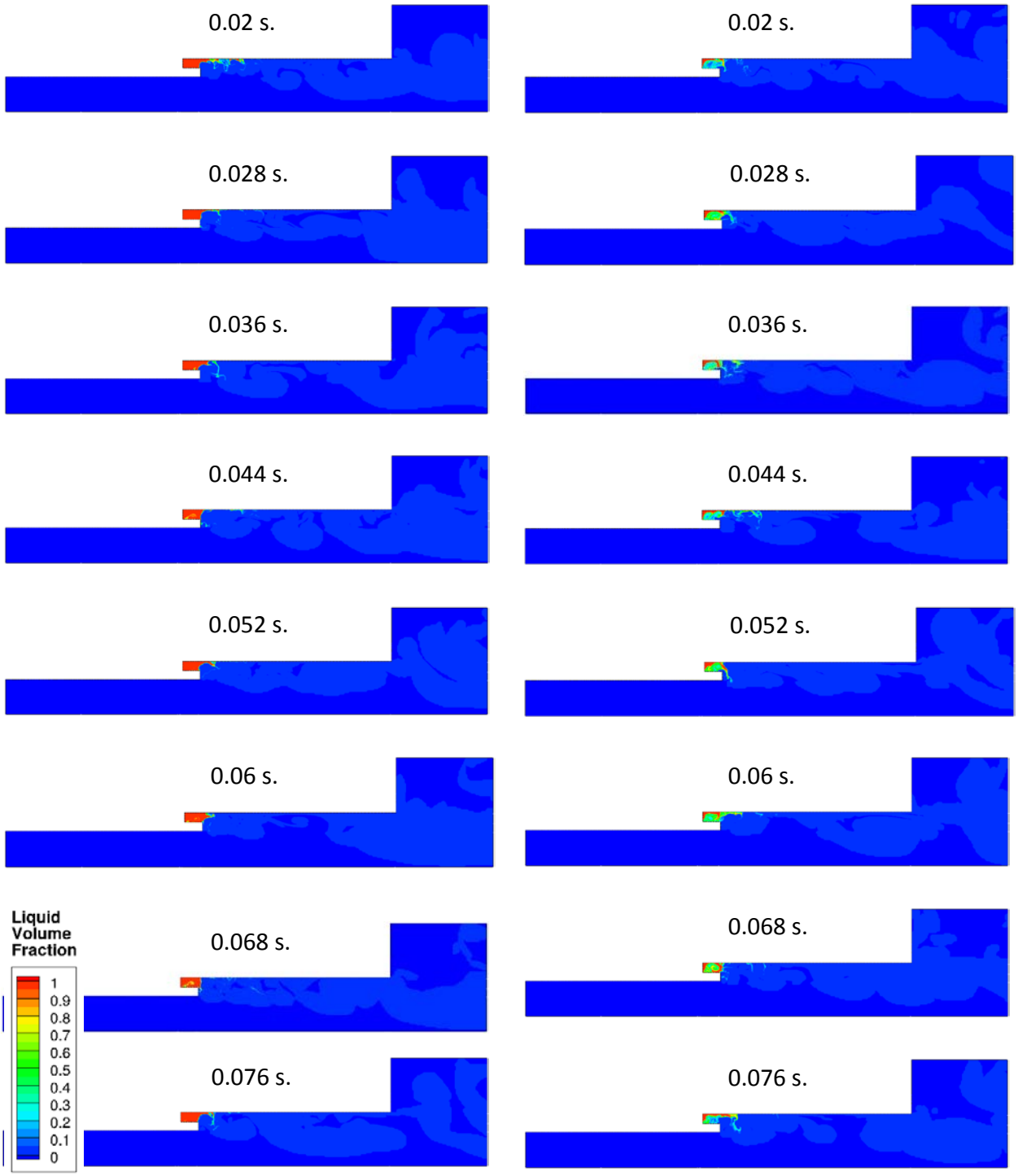

Figure 9. Contours of Liquid Volume Fraction. K-omega Turbulence Model.
No Swirl versus Swirl, mg = 0.0567 kg/s, ml=0.0327 kg/s, Vs ~ 3.9 m/s., Po ~ 104 kPa (MFR ~ 270)

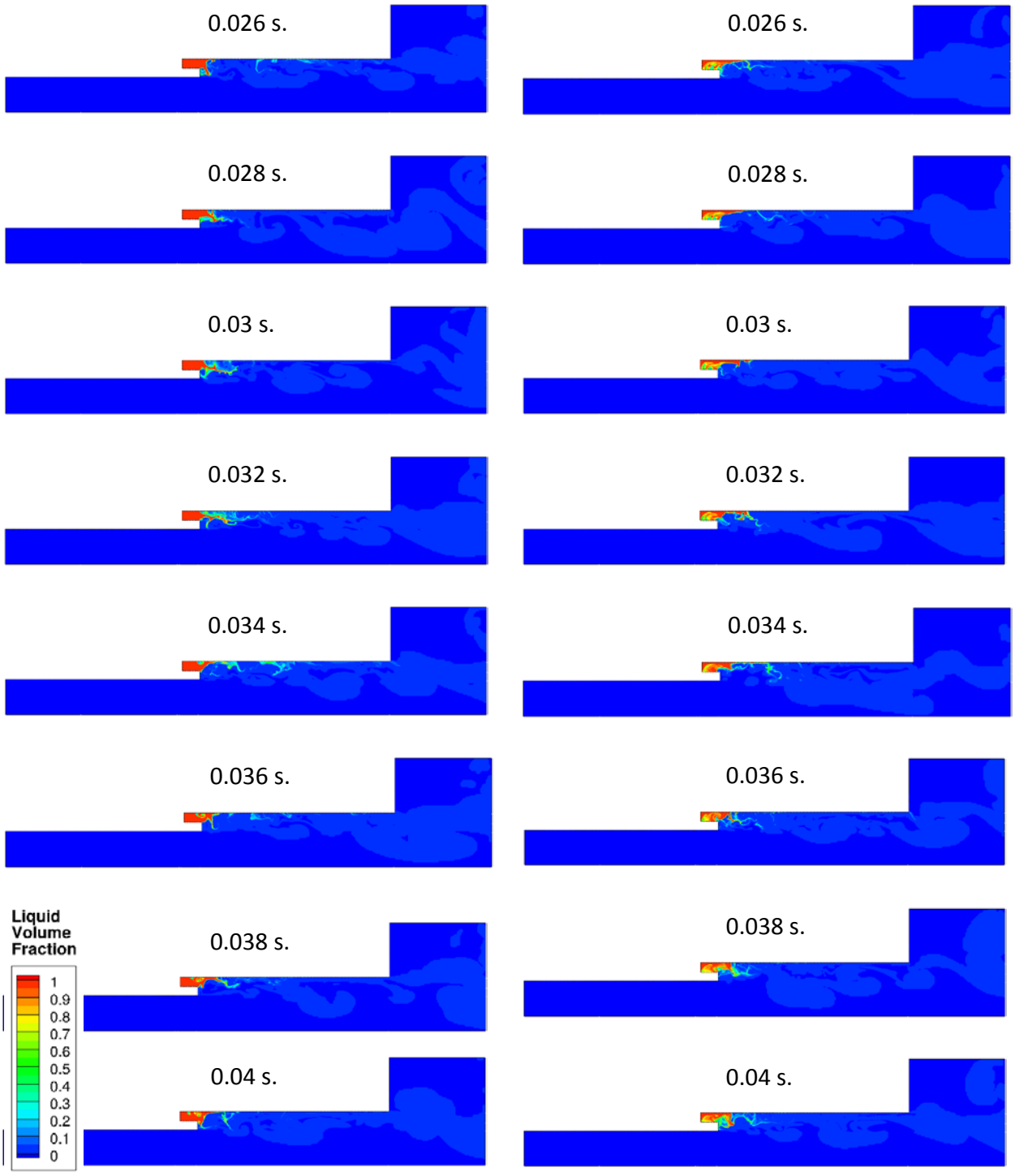

Figure 10. Contours of Liquid Volume Fraction. RSM turbulence model with SWF treatment predictions. No Swirl versus Swirl, mg = 0.0567 kg/s, ml=0.0327 kg/s, Vs ~ 3.9 m/s., Po ~ 104 kPa (MFR ~ 270)

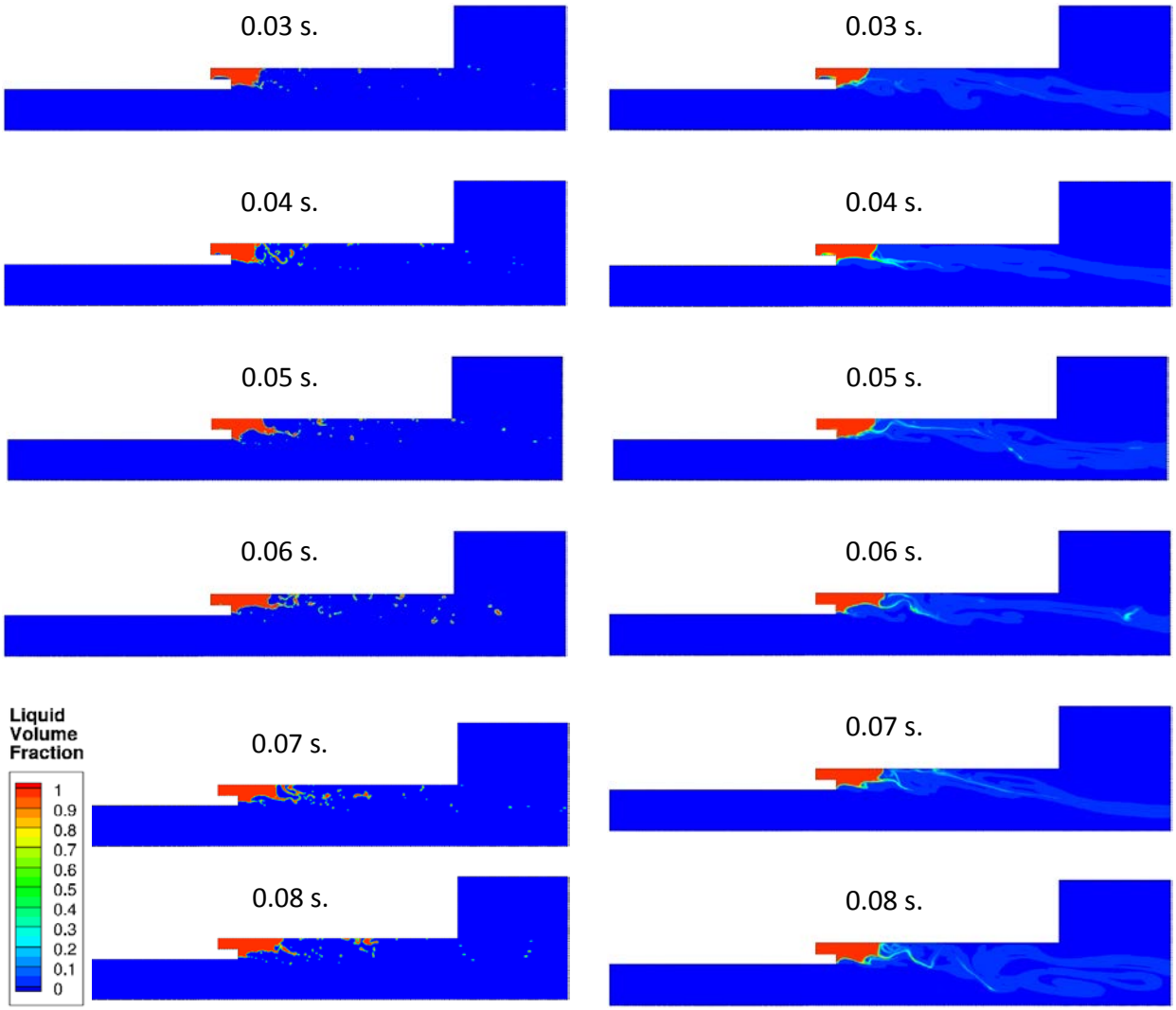

Figure 11. Contours of Liquid Volume Fraction. K-epsilon Turbulence Model.
Geo-Reconstruct versus Second Order Upwind Discretization.
mg = 0.0567 kg/s, ml=0.0327 kg/s, Vs ~ 3.9 m/s., Po ~ 104 kPa (MFR ~ 270)